Terahertz spectroscopy of spin waves in multiferroic $BiFeO_3$ in high magnetic fields

U. Nagel,[1,*] T. Katuwal,[1,†] H. Engelkamp,[2] D. Talbayev,[3] Hee Taek Yi,[4] S.-W. Cheong,[4] and T. Rõõm[1]

[1] *National Institute of Chemical Physics and Biophysics, Akadeemia tee 23, 12618 Tallinn, Estonia*
[2] *Radboud University Nijmegen, Institute for Molecules and Materials, High Field Magnet Laboratory, Toernooiveld 7, 6525 ED Nijmegen, the Netherlands*
[3] *Department of Physics, Tulane University, 5032 Percival Stern Hall, New Orleans, LA 70118, USA*
[4] *Rutgers Center for Emergent Materials and Department of Physics and Astronomy, Rutgers University, 136 Frelinghuysen Rd., Piscataway, New Jersey 08854, USA*

(Dated: February 12, 2013)

We have studied the magnetic field dependence of far-infrared active magnetic modes in a single ferroelectric domain $BiFeO_3$ crystal at low temperature. The modes soften close to the critical field of 18.8 T along the [001] (pseudocubic) axis, where the cycloidal structure changes to the homogeneous canted antiferromagnetic state and a new strong mode with linear field dependence appears that persists at least up to 31 T. This allows us to assign the low field modes to the excitations of the cycloid and the high field mode to the antiferromagnetic resonance. We found that the zero field spectra at low temperature are different before and after application of high magnetic field and this change persists at low temperature. We interpret this as a change from a state with three magnetic domains into a state with one domain with the lowest energy in high magnetic field.

PACS numbers: 75.85.+t, 76.50.+g, 78.30.-j

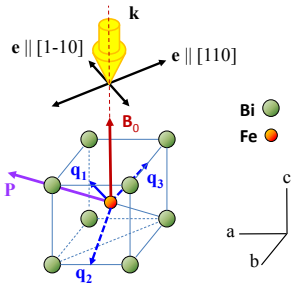

FIG. 1. (color online) Pseudocubic unit cell of $BiFeO_3$ showing the positions of Bi and Fe ions, the ferroelectric polarization **P**, three equivalent directions of the cycloidal ordering vector $\mathbf{q}_i$, the applied static magnetic field $\mathbf{B}_0 \parallel [001]$, and the wave vector of incident light **k** together with the electric field (**e**) component of light in two orthogonal polarizations that were used in the experiment.

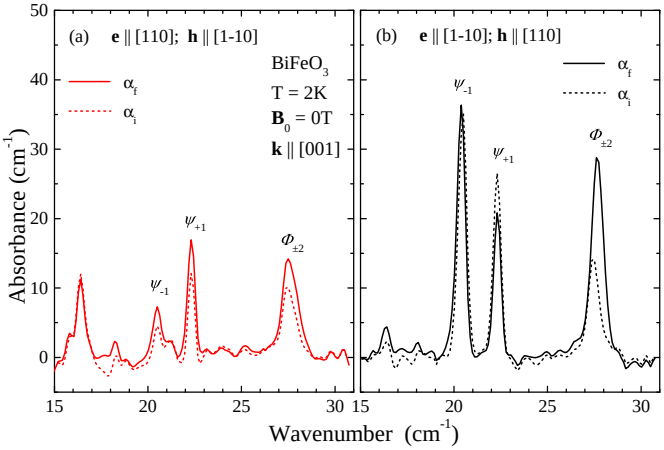

FIG. 2. (color online) Absorbance spectra of cycloid modes in zero field and in $\mathbf{e} \parallel [110]$ polarization (a) and in $\mathbf{e} \parallel [1\bar{1}0]$ polarization (b). Solid curves, α_F, were measured after applying the high field $\mathbf{B}_0 \geq 21$ T. Dotted curves are initial absorbance spectra α_I of the zero field cooled sample.

Multiferroics are materials with more than one ferroic order parameter and they have been in the focus of recent research [1–7]. Among multiferroics $BiFeO_3$ is the only known one that exhibits both ferroelectric and magnetic orders already at room temperature. Below $T_{\mathrm{Curie}} \approx 1100$ K it has a rhombohedrally distorted perovskite structure [8], space group R3c, were the iron (Fe^{3+}) and bismuth (Bi^{3+}) cations are displaced from their centrosymmetric positions and produce a polar distortion, resulting in a spontaneous ferroelectric polarization **P** along the [111] direction of the pseudocubic unit cell [9].

$BiFeO_3$ shows G-type antiferromagnetic (AFM) order below $T_N \approx 640$ K in which the Fe^{3+} magnetic moments are ordered antiferromagnetically between adjacent pseudocubic (111) planes [10, 11]. Ferromagnetic ordering within the planes is broken by a long-wavelength cycloidal spin order [11] with three possible directions of the ordering vector $\mathbf{q}_i \,||\, \{[1,\bar{1},0],[0,1,\bar{1}],[\bar{1},0,1]\} \perp \mathbf{P}$, see Fig. 1. The spins of a cycloid $\mathbf{q}_i$ are in the plane determined by **P** and $\mathbf{q}_i$.

The cycloidal order in $BiFeO_3$ is induced by a weak relativistic Dzyaloshinskii-Moriya interaction with coupling constant $\mathbf{D}_c \perp \mathbf{P}$ and $\mathbf{D}_c \perp \mathbf{q}_i$ [12]. Another Dzyaloshinskii-Moriya interaction $\mathbf{D} \parallel [111]$ cants spins out of the cycloid plane [3, 12] and the ferromagnetic ordering of this canted moment has been verified by a neutron scattering experiment [13]. High resolution neutron scattering shows that the magnetic ground state ordering in $BiFeO_3$ does not change in zero field on cooling from

TABLE I. Fitted positions and areas of absorption lines from Fig. 2. A_i and A_f are the line areas before and after application of $B_0 > 21\,\mathrm{T}$. Fit errors are three times standard error. Mode labels are according to Fishman et al. [27]. The Φ_{-1} mode position is an extrapolated value of the magnetic field dependence to 0 T, Fig.4. $A_{\mathbf{q}_1}$ and $A_{\mathbf{q}_{1,2,3}}$ are theoretical line areas in arbitrary units assuming a magnetic monodomain with $\mathbf{q}_1$ and an equal population of $\mathbf{q}_1$, $\mathbf{q}_2$ and $\mathbf{q}_3$ domains, respectively. The line areas of three modes are $\Psi_{-1} : A = \sum_i n_i |\langle q_i|M_{z_i}|0\rangle|^2 h_{z_i}^2$, $\Psi_{+1} : A = \sum_i n_i [|\langle q_i|M_{x_i}|0\rangle|^2 h_{x_i}^2 + |\langle q_i|P_{y_i}|0\rangle|^2 e_{y_i}^2]$, $\Phi_{\pm 2} : A = \sum_i n_i |\langle q_i|M_{y_i}|0\rangle|^2 h_{y_i}^2$, where $\mathbf{x}_i \parallel \mathbf{q}_i$, $\mathbf{z}_i \parallel [111]$ and $\mathbf{y}_i = \mathbf{z}_i \times \mathbf{x}_i$, populations $n_1 + n_2 + n_3 = 1$ and $|\mathbf{h}| = |\mathbf{e}| = 1$. Matrix elements are [27] $|\langle q_i|M_{x_i}|0\rangle| = 4, |\langle q_i|M_{y_i}|0\rangle| = 0.8, |\langle q_i|M_{z_i}|0\rangle| = 3.6$ at $K = 0.002\,\mathrm{meV}$, $p = |\langle q_i|P_{y_i}|0\rangle|$.

	$\mathbf{e} \parallel [110]$					$\mathbf{e} \parallel [1\bar{1}0]$				
Mode	center / cm^{-1}	A_f / cm^{-2}	A_i / cm^{-2}	$A_{\mathbf{q}_1}$	$A_{\mathbf{q}_{1,2,3}}$	center / cm^{-1}	A_f / cm^{-2}	A_i / cm^{-2}	$A_{\mathbf{q}_1}$	$A_{\mathbf{q}_{1,2,3}}$
Φ_{-1}	11.0 ± 0.1	-	-			-	-	-		
Ψ_0, Φ_{+1}	16.38 ± 0.05	6.9 ± 1.0	6.9 ± 2.0			16.35 ± 0.09	1.3 ± 0.6	0.9 ± 0.7		
	18.24 ± 0.12	0.8 ± 0.6	0.8 ± 1.6			18.05 ± 0.18	0.3 ± 0.5	-		
Ψ_{-1}	20.53 ± 0.08	4.7 ± 1.0	2.1 ± 1.8	0	0	20.37 ± 0.01	21.0 ± 0.8	20.0 ± 0.8	8.6	8.6
Ψ_{+1}	22.32 ± 0.02	8.4 ± 0.9	4.1 ± 1.6	$16 + p^2/3$	$8 + p^2/6$	22.31 ± 0.02	10.5 ± 0.8	13.9 ± 0.8	0	$2.7 + p^2/2$
$\Phi_{\pm 2}$	27.58 ± 0.04	14.3 ± 1.3	9.1 ± 2.1	0	0.32	27.67 ± 0.02	23.5 ± 0.7	11.5 ± 1.0	0.21	0.11

300 K to 4 K [14–16].

Single ion anisotropy along the easy axis [111] introduces anharmonicity [12, 17], but in zero magnetic field the cycloid is only slightly anharmonic [16, 18]. External magnetic field contributes to the effective single ion anisotropy [19] and induces a metamagnetic transition [12] at a critical field $B_c \approx 19\,\mathrm{T}$, where the cycloidal order changes to a collinear AFM spin order [20]. The unwinding of the cycloid reduces the electric polarization [21] and creates a small macroscopic spontaneous magnetization induced by $\mathbf{D} \parallel [111]$ [12, 21].

In $BiFeO_3$ it has been shown that electric field flips polarization $\mathbf{P}$ together with the cycloidal plane and changes the populations of magnetic domains [22–24]. To our best knowledge there is no information whether the applied magnetic field reorients magnetic domains in a single crystals or not, although the simultaneous action of electric and magnetic, internal or external fields, is crucial in the operation of exchange-biased devices [25].

The eigenfrequencies of magnetic modes are sensitive to anisotropic magnetic interactions and these interactions are important to understand the microscopic models behind magneto-electric coupling in multiferroics. The eigenspectrum of $BiFeO_3$ cycloids was calculated by de Sousa and Moore [26] and with the addition of single-ion easy-axis anisotropy by Fishman et al.[27] in 0 T and in applied electric field by Rovillain et al.[28]. Spectroscopic techniques what measure the eigenspectrum of magnetic modes, especially if they can be combined with external fields what compete with internal fields, are valuable tools. Most of the INS [29, 30], Raman [31, 32] and THz [33, 34] spectroscopy studies on $BiFeO_3$ were in zero applied field. The Raman work demonstrated that the Raman-active magnon frequencies depend strongly on applied electric field [28]. The high field ESR was done in magnetic fields up to 25 T, but was limited to frequencies lower than the main cycloid modes and one of the AFM modes.

In this work, we present THz spectra of $BiFeO_3$ single crystals at low temperature and $B_0 \leq 31\,\mathrm{T}$ which allow us to identify the excitations of the cycloid and follow their magnetic field dependence until the cycloidal order is destroyed in high magnetic field. We show that magnetic field changes the distribution of magnetic domains.

The (001) face single crystal $BiFeO_3$ sample was grown using a Bi_2O_3 flux [35]. It has a thickness of 0.37 mm and it contains a single ferroelectric domain along the [111] axis, Fig. 1, checked by an optical rectification experiment [36].

The sample was zero field cooled and spectra were measured in Faraday configuration with the magnetic field along the [001] axis. Up to 12 T spectra were measured at 4 K in Tallinn with a Martin-Puplett spectrometer and a 0.3 K bolometer [37] using a spectral resolution of $0.2\,\mathrm{cm}^{-1}$. Spectra from 12 T up to 31 T were measured in Nijmegen High Field Magnet Laboratory at 2 K using a Bruker IFS 113v spectrometer and a 1.6 K silicon bolometer and spectral resolution of $0.43\,\mathrm{cm}^{-1}$; the spectra were averaged for 15 minutes at each field. There was a linear polarizer in front of the sample to control the polarization of light.

We measured absorbance spectra in magnetic field with the reference spectrum in zero field. This method gave excellent spectra of magnetic field dependent lines. From the relative absorbance spectra in fields above 21 T (after applying 30 T) we extracted the zero field absorption lines, solid curves in Fig. 2 and fitted them. The zero field fit results, parameters in Table I, were added to the measured relative spectra in magnetic fields. The result, absolute absorbance spectra in fields, are shown in Fig. 3, and fitted line positions and areas in Fig. 4.

We observed a change in the zero field spectra after applying high field at low temperature, Fig. 2. The zero field spectrum stayed the same after applying high field in the opposite direction. The initial zero field line intensities α_I, measured on the zero field cooled sample, were recovered after warming the sample to 300 K. This is an evidence that different magnetic domains exist.

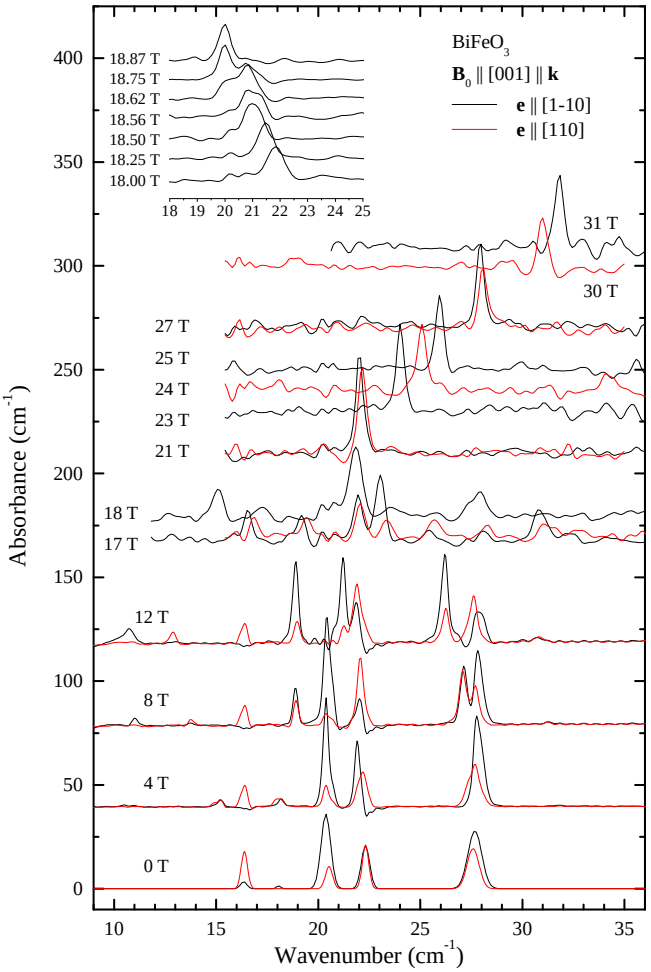

FIG. 3. (color online) Magnetic field dependence of absorbance spectra of $BiFeO_3$ in $\mathbf{e} \parallel [1\bar{1}0]$ (black) and $\mathbf{e} \parallel [110]$ (red) polarizations. Zero field spectra are fits as described in the text. The inset shows a detailed view in the spectral range of the AFM resonance close to the metamagnetic transition, $B_c = 18.8\,\mathrm{T}$.

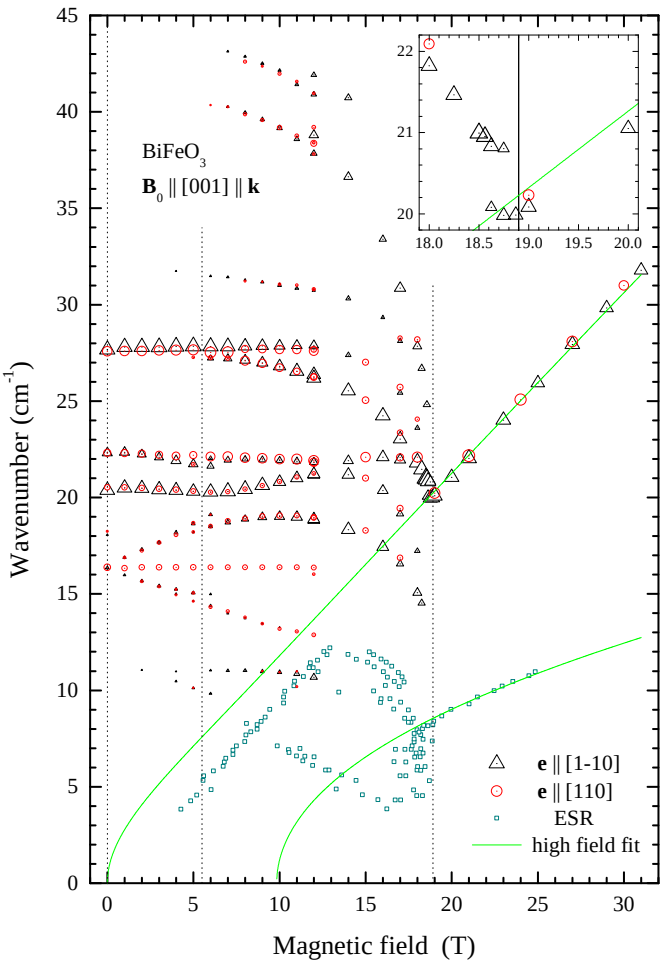

FIG. 4. (color online) Magnetic field dependence of magnon modes in the THz spectrum of $BiFeO_3$ at low temperature. The areas of triangles and circles are proportional to the absorption line areas. Vertical dashed lines mark the metamagnetic transition at $B_c = 18.8\,\mathrm{T}$ and another critical field $B_a \approx 5.5\,\mathrm{T}$. The solid lines are the fit of our data and ESR data [38] (squares) above 19 T to a model from Ref. 38.

When the cycloidal order is destroyed above the critical field B_c a collinear AFM order is established where the spins are in the (111) plane [20] with moments $\mathbf{M}_1$ and $\mathbf{M}_2$ antiparallel in neighboring planes and with a small canted moment in the (111) plane, $\mathbf{M} = \mathbf{M}_1 + \mathbf{M}_2$, induced by $\mathbf{D} \parallel [111]$ [3, 12]. The energy is at the minimum when $\mathbf{M} \parallel \mathbf{B}_0$ and for the field $[0, 0, B_0]$ this happens for the $\mathbf{q}_1$ domain and the AFM vector $\mathbf{L} = \mathbf{M}_1 - \mathbf{M}_2$ will be aligned along $\mathbf{q}_1$. Even if the high field is removed, the selected $\mathbf{q}$ will remain and a monodomain cycloidal state is created.

We found that the change in the zero field spectra occurs already by 12 T and higher fields that destroy the cycloid do not change the zero field lines any more. Apparently the $\mathbf{q}_1$ cycloid where the field is mostly perpendicular to the cycloid plane has a lower energy than the cycloids $\mathbf{q}_2$ and $\mathbf{q}_3$ where the magnetic field is closer to the cycloid planes. This means that a net magnetic moment perpendicular to the cycloid plane is created by applied field. Indeed, a non-linear dependence of $M(B_0)$ has been observed below 5 T if the direction of $\mathbf{B}_0$ deviates from the [111] direction [21]. The results shown in Fig. 3 and 4 were obtained from spectra measured after the sample had been in high field $\geq 12\,\mathrm{T}$ and in further discussion we assume that $\mathbf{q}_1$ is the only cycloid present.

The zero field line parameters are compared to the calculation of Fishman et al.[27] in Table I using their notation for the cycloid modes. The largest absorption line area is that of the $\Phi_{\pm 2}$ line in $\mathbf{e} \parallel [1\bar{1}0]$ polarization and it is quite strong also in the other polarization, contrary to the theory what predicts the smallest matrix element among magnetic dipole transitions for this mode. The polarization dependence of the Ψ_{-1} and Ψ_{+1} modes is

better described by the calculation.

The spectra in field and a detailed field dependence of mode frequencies and areas are presented in Fig. 3 and 4. We see that more modes, too weak to be detected in zero field, coincide with modes predicted in Ref. 27: $11\,\mathrm{cm}^{-1}$ with Φ_{-1} and $32\,\mathrm{cm}^{-1}$ with $\Psi_{\pm 2}$ mode at $q = 2$, and the two modes between 40 and $45\,\mathrm{cm}^{-1}$ are even higher order excitations.

The three main modes, Ψ_{-1}, Ψ_{+1} and $\Phi_{\pm 2}$ change only slightly with increasing magnetic field until a critical field $B_a \approx 5.5\,\mathrm{T}$ is reached, where a discontinuity on several modes and a smooth change in the slope of the Ψ_{+1} mode is observed, Fig. 4. These changes might be associated with the change in the magnetic structure. Indeed, the magnetization measurements on similar samples show a non-linear behavior of $M(B_0)$ below 5 T and almost linear behavior above [21]. However, the THz spectra do not show any anomalies at 10 T seen by optical measurements [39].

Modes soften before reaching the metamagnetic transition at B_c, except Ψ_{+1} which seems to merge with the softening $\Phi_{\pm 2}$ at about 18 T. There is an intriguing possibility that close to transition between 18.6 and 18.8 T, see inset to Fig. 3 and 4, one of the cycloid resonances, Ψ_{+1} or $\Phi_{\pm 2}$ as labeled in zero field, coexists with the AFM resonance. This means that in a narrow field interval the spin structure supports both, cycloid-like and AFM-like mode. The coexistence of two phases is ruled out since the metamagnetic transition in $BiFeO_3$ is not the first order phase transition nor similar to a spin flop transition in ordinary antiferromagnets [19] and we did not observe any hysteresis effects between 18 and 19 T as reported earlier [38]. In THz spectra there is only one resonance line above 18.8 T and we assign this value to the critical field B_c of the metamagnetic transition in $BiFeO_3$ at 2 K and $\mathbf{B}_0 \parallel [001]$.

From the ESR [38] and THz spectra we have both AFM resonances in hand and we fit them to the model described in [38]. The magnetic field $\mathbf{B}_0$ projected on the axes of the $\mathbf{q}_1$ cycloid is $B_0[0, \sqrt{2/3}, \sqrt{1/3}]$. We get the following parameters: gyromagnetic ratio $\gamma = (1.72 \pm 0.01) \times 10^7\,\mathrm{rad(s\,Oe)}^{-1}$, $K_u/\chi_\perp = (1.06 \pm 0.02) \times 10^{10}\,\mathrm{erg/cm}^3$, $H_{DM} = (105 \pm 2)\mathrm{kOe}$, see the solid lines in Fig. 4. K_u is the uniaxial magnetic anisotropy constant and $\chi_\perp$ is the susceptibility perpendicular to the $\mathbf{L}$. The canted moment $\chi_\perp H_{DM} = \mathbf{M}_1 + \mathbf{M}_2$ is induced by $\mathbf{D}$. We use $\chi_\perp = 3.1 \times 10^{-5}$ from the high field magnetization measurement [21] and get for the magnetic anisotropy constant (energy density) $K_u = 3.3 \times 10^5\,\mathrm{erg\ cm}^{-3}$. We get for the same quantity $\langle K S_z^2 \rangle = 3.2 \times 10^5\,\mathrm{erg\ cm}^{-3}$ from the microscopic model [27] where $K = 0.002\,\mathrm{meV}$ and assuming $S_z = 5/2$. The canted moment estimated from the AFM resonance spectra is $\chi_\perp H_{DM} = 0.022\mu_B/\mathrm{Fe}$. This should be compared to $0.05\mu_B$ derived from the interpolation of the high field magnetization to the zero field ($0.04\mu_B$/Fe projected on $[0, \sqrt{2/3}, \sqrt{1/3}]$ direction) [21] and to averaged local magnetization $0.06\mu_B$/Fe in the cycloidal phase [16].

In summary, the cycloid modes soften close to the metamagnetic transition at $B_c = 18.8\,\mathrm{T}$ and are replaced by two AFM modes, one observed earlier by ESR [38]. The parameters derived from the AFM resonances are in reasonable agreement with neutron scattering [16] and magnetization [21] measurements and with the microscopic spin model [27]. This model describes properly the resonance frequencies of the cycloid modes in zero magnetic field. However, the assumption that these transitions are only magnetic dipole active is not sufficient to account for the observed polarization dependence. Theory is needed to describe the $\mathbf{B}_0$ dependence of the cycloid excitations and the observed discontinuity of mode dispersion in magnetic field at 5.5 T calls for the need to revise the minimal magnetic model in $BiFeO_3$. Our work demonstrates that in addition to electric field [23] the control of magnetic domains with magnetic field is possible; a neutron scattering experiment where both fields are applied is needed to understand multiferroic properties of $BiFeO_3$.

We acknowledge support by the Estonian Ministry of Education and Research grant No. SF0690029s09, Estonian Science Foundation grant Nos. ETF8170, ETF8703 and ERMOS67, and by EuroMAgNET under the EU Contract No. 228043. Work at Rutgers was supported by NSF-DMR-1104484.

* urmas.nagel@kbfi.ee
† On leave from Department of Physics, Trichandra College, Tribhuvan University, Kathmandu, Nepal

[1] N. A. Hill, J. Phys. Chem. B **104**, 6694 (2000).
[2] M. Fiebig, J. Phys. D: Appl. Phys. **38**, R123 (2005).
[3] C. Ederer and N. A. Spaldin, Phys. Rev. B **71**, 060401 (2005).
[4] W. Eerenstein, N. D. Mathur, and J. F. Scott, Nature **442**, 759 (2006).
[5] S.-W. Cheong and M. Mostovoy, Nature Mater. **6**, 13 (2007).
[6] D. Khomskii, Physics **2**, 20 (2009).
[7] N. A. Spaldin, S.-W. Cheong, and R. Ramesh, Physics Today **63**, 38 (2010).
[8] C. Michel, J.-M. Moreau, G. D. Achenbach, R. Gerson, and W. J. James, Solid State Commun. **7**, 701 (1969).
[9] J. R. Teague, R. Gerson, and W. J. James, Solid State Commun. **8**, 1073 (1970).
[10] S. V. Kiselev, R. P. Ozerov, and G. S. Zhdanov, Sov. Phys.-Dokl. **7**, 724 (1963).
[11] I. Sosnowska, T. Peterlin-Neumaier, and E. Steichele, J. Phys. C: Solid State Phys. **15**, 4835 (1982).
[12] A. M. Kadomtseva, A. K. Zvezdin, Y. P. Popov, A. P. Pyatakov, and G. P. Vorobev, JETP Lett. **79**, 571 (2004).
[13] M. Ramazanoglu, M. Laver, W. Ratcliff, S. M. Watson, W. C. Chen, A. Jackson, K. Kothapalli, S. Lee, S.-W. Cheong, and V. Kiryukhin, Phys. Rev. Lett. **107**, 207206

(2011).
[14] R. Przeniosło, A. Palewicz, M. Regulski, I. Sosnowska, R. M. Ibberson, and K. S. Knight, J. Phys.: Condens. Matter **18**, 2069 (2006).
[15] J. Herrero-Albillos, G. Catalan, J. A. Rodriguez-Velamazan, M. Viret, D. Colson, and J. F. Scott, J. Phys.: Condens. Matter **22**, 256001 (2010).
[16] M. Ramazanoglu, W. Ratcliff, Y. J. Choi, S. Lee, S.-W. Cheong, and V. Kiryukhin, Phys. Rev. B **83**, 174434 (2011).
[17] A. M. Kadomtseva, Y. P. Popov, A. P. Pyatakov, G. P. Vorob'ev, A. K. Zvezdin, and D. Viehland, Phase Transitions **79**, 1019 (2006).
[18] I. Sosnowska and R. Przeniosło, Phys. Rev. B **84**, 144404 (2011).
[19] M.-M. Tehranchi, N. F. Kubrakov, and A. K. Zvezdin, Ferroelectrics **204**, 181 (1997).
[20] K. Ohoyama, S. Lee, S. Yoshii, Y. Narumi, T. Morioka, H. Nojiri, G. S. Jeon, S.-W. Cheong, and J.-G. Park, J. Phys. Soc. Jpn. **80**, 125001 (2011).
[21] J. Park, S.-H. Lee, S. Lee, F. Gozzo, H. Kimura, Y. Noda, Y. J. Choi, V. Kiryukhin, S.-W. Cheong, Y. Jo, E. S. Choi, L. Balicas, G. S. Jeon, and J.-G. Park, J. Phys. Soc. Jpn. **80**, 114714 (2011).
[22] D. Lebeugle, D. Colson, A. Forget, M. Viret, A. M. Bataille, and A. Gukasov, Phys. Rev. Lett. **100**, 227602 (2008).
[23] S. Lee, W. Ratcliff, S.-W. Cheong, and V. Kiryukhin, Appl. Phys. Lett. **92**, 192906 (2008).
[24] S. Lee, T. Choi, W. Ratcliff, R. Erwin, S.-W. Cheong, and V. Kiryukhin, Phys. Rev. B **78**, 100101 (2008).
[25] S. M. Wu, S. A. Cybart, D. Yi, J. M. Parker, R. Ramesh, and R. C. Dynes, Phys. Rev. Lett. **110**, 067202 (2013).
[26] R. de Sousa and J. E. Moore, Phys. Rev. B **77**, 012406 (2008).
[27] R. S. Fishman, N. Furukawa, J. T. Haraldsen, M. Matsuda, and S. Miyahara, Phys. Rev. B **86**, 220402 (2012).
[28] P. Rovillain, R. d. Sousa, Y. Gallais, A. Sacuto, M. A. Méasson, D. Colson, A. Forget, M. M. Bibes, A. Barthélémy, and M. Cazayous, Nature Mater. **9**, 975 (2010).
[29] J. Jeong, E. A. Goremychkin, T. Guidi, K. Nakajima, G. S. Jeon, S.-A. Kim, S. Furukawa, Y. B. Kim, S. Lee, V. Kiryukhin, S.-W. Cheong, and J.-G. Park, Phys. Rev. Lett. **108** (2012).
[30] M. Matsuda, R. S. Fishman, T. Hong, C. H. Lee, T. Ushiyama, Y. Yanagisawa, Y. Tomioka, and T. Ito, Phys. Rev. Lett. **109**, 067205 (2012).
[31] M. Cazayous, Y. Gallais, A. Sacuto, R. de Sousa, D. Lebeugle, and D. Colson, Phys. Rev. Lett. **101**, 037601 (2008).
[32] P. Rovillain, M. Cazayous, Y. Gallais, A. Sacuto, R. P. S. M. Lobo, D. Lebeugle, and D. Colson, Phys. Rev. B **79**, 180411 (2009).
[33] G. A. Komandin, V. I. Torgashev, A. A. Volkov, O. E. O. E. Porodinkov, I. E. Spektor, and A. A. Bush, Physics of the Solid State **52**, 734 (2010).
[34] D. Talbayev, S. A. Trugman, S. Lee, H. T. Yi, S.-W. Cheong, and A. J. Taylor, Phys. Rev. B **83**, 094403 (2011).
[35] T. Choi, S. Lee, Y. J. Choi, V. Kiryukhin, and S.-W. Cheong, Science **324**, 63 (2009).
[36] D. Talbayev, A. D. LaForge, S. A. Trugman, N. Hur, A. J. Taylor, R. D. Averitt, and D. N. Basov, Phys. Rev. Lett. **101**, 247601 (2008).
[37] T. Rõõm, D. Hüvonen, U. Nagel, Y.-J. Wang, and R. K. Kremer, Phys. Rev. B **69**, 144410 (2004).
[38] B. Ruette, S. Zvyagin, A. P. Pyatakov, A. Bush, J. F. Li, V. I. Belotelov, A. K. Zvezdin, and D. Viehland, Phys. Rev. B **69**, 064114 (2004).
[39] X. S. Xu, T. V. Brinzari, S. Lee, Y. H. Chu, L. W. Martin, A. Kumar, S. McGill, R. C. Rai, R. Ramesh, V. Gopalan, S. W. Cheong, and J. L. Musfeldt, Phys. Rev. B **79**, 134425 (2009).